Contents lists available at NCBI

The American Journal of Science and Medical Research

Journal homepage: https://ajsmrjournal.com/

Research Article

# Structure-Based Discovery of Phytochemical Inhibitors Targeting Cytochrome P450 17A1 (CYP17A1) For Prostate Cancer therapy

Madhav Morla[1], Estari Mamidala[2]*

[1] Department of Biochemistry, Kakatiya University, Warangal-506009 Telangana State, India
[3] Department of Zoology, Kakatiya University, Warangal-506009 Telangana State, India

*Corresponding author:
E-mail: *drestari@kakatiya.ac.in;
https://orcid.org/0000-0002-7874-6019
madhavmorla29@gmail.com;
https://orcid.org/0009-0002-0346-898X

https://dx.doi.org/10.5281/zenodo.21386532

*Received: 19 December 2025*
*Accepted: 21 January 2026*
*Published: 26 January 2026*

ISSN: 2377-6196© 2025 The Authors.
*Published by AIRA*

**Keywords:** *Prostate cancer, CYP17A1, phytochemicals, molecular docking, drug discovery*

## ABSTRACT

Prostate cancer is one of the most prevalent malignancies affecting men worldwide and is strongly associated with androgen biosynthesis. The enzyme cytochrome P450 17A1 (CYP17A1) plays a critical role in the production of androgens and represents an important therapeutic target for prostate cancer treatment. In the present study, a structure-based computational approach was employed to identify potential phytochemical inhibitors targeting CYP17A1. The three-dimensional crystal structure of CYP17A1 (PDB ID: 6WR1) was retrieved from the Protein Data Bank and used for molecular docking analysis. A library of selected phytochemicals obtained from natural sources was screened against the active site of the enzyme to evaluate their binding affinity and interaction patterns. The docking results revealed that several phytochemicals exhibited strong binding interactions with key residues within the catalytic pocket of CYP17A1. Among the screened compounds, IMPHY009079 showed the highest binding affinity with a docking score of −11.39 kcal·mol$^{-1}$ and an estimated inhibition constant (Ki) of approximately 4.96 nM, indicating strong inhibitory potential. This compound formed hydrogen bonds with important residues such as HIS373, ILE371, and ARG96, along with extensive hydrophobic interactions involving LEU370, CYS442, VAL310, and PHE435, contributing to the stability of the ligand–protein complex. Other phytochemicals, including IMPHY008870 and IMPHY007444, also demonstrated notable binding affinities with docking scores of −10.01 kcal·mol$^{-1}$ and −9.91 kcal·mol$^{-1}$, respectively, suggesting stable interactions within the active site of the enzyme. These findings highlight several promising phytochemical leads that may act as potential CYP17A1 inhibitors. The identified compounds could serve as valuable candidates for further optimization and experimental validation in the development of novel plant-derived therapeutics for prostate cancer management.

## 1. Introduction

Prostate cancer is one of the most prevalent malignancies among men worldwide and Epidemiological data indicate that the disease burden continues to rise, with age-standardized incidence rates highest in developed regions. According to global cancer statistics, prostate cancer accounts for nearly 15% of cancer diagnoses in men, with incidence rates continuing to rise, particularly in aging populations (Filho et al., 2025) (Schafer et al., 2025). The disease is predominantly driven by androgen signalling, which plays a crucial role in the development, differentiation, and survival of prostate cells. Androgens stimulate cell proliferation and tumour growth through the AR signalling pathway. Because of this, therapeutic strategies have traditionally focused on disrupting androgen biosynthesis or inhibiting AR activation, thereby depriving cancer cells of the signals required for continued growth and survival(Rebello et al., 2021; Lunavath et al., 2015).

Prostate cancer treatment continues to focus on disrupting the androgen receptor, androgen deprivation therapy (ADT) and agents that block androgen synthesis such as CYP17A1 inhibitors (e.g., abiraterone). The Cytochrome P450 17A1 (CYP17A1) plays a central role in androgen biosynthesis. carrying out both 17α-hydroxylase and 17,20-lyase reactions that convert pregnenolone and progesterone into androgen precursors. Through these steps, tightly regulates both intratumoral and systemic androgen levels. Elevated expression or enhanced activity of CYP17A1 has been closely

linked to disease progression, particularly in castration-resistant prostate cancer (CRPC), where tumours continue to sustain androgen receptor (AR) signalling despite reduced circulating androgen levels. Because of its pivotal role in maintaining androgen production under such conditions, CYP17A1 is widely recognized as a well-validated and promising therapeutic target (Kmeťová Sivoňová et al., 2017)(Wróbel et al., 2022).
Clinically, inhibition of CYP17A1 with agents such as abiraterone has improved outcomes for patients with metastatic CRPC by further reducing androgen synthesis and attenuating AR signalling (Petrunak et al., 2023). Given these challenges, there is growing interest in identifying novel phytochemical inhibitors of CYP17A1. phytochemicals often offer structural diversity and favourable safety profiles, making them promising starting points for drug discovery. Structure-based approaches such as molecular docking enable rapid in silico screening of large compound libraries to predict binding modes, estimate affinities, and prioritize candidates for experimental validation (Alex et al., 2016) (Omoboyowa et al., 2022; Kumar et al., 2020; Porika et al., 2014; Kumar et al., 2017).

This study is dedicated to the structure-based identification of phytochemical inhibitors targeting CYP17A1, using molecular docking simulations as the primary approach, with abiraterone serving as the reference inhibitor (Mortezavi et al., 2019). has demonstrated clinical efficacy, but structural analogs may offer enhanced binding affinity and pharmacokinetic properties. By analysing binding energies, interaction patterns, and pharmacophore features, this in silico investigation seeks to uncover promising candidates for further experimental validation. Beyond identifying new phytochemical inhibitors, this exploration of phytochemicals enhances our understanding of their molecular behaviour and contributes to the broader vision of plant-based precision oncology. By harnessing nature-inspired scaffolds and refining them through computational and structural biology, researchers can develop targeted, sustainable, and safer strategies for cancer therapy (Omoboyowa et al., 2022; Poojari et al., 2014; Mamidala et al., 2020).

## 2. Materials and Methods

### 1.1 Selection of Target Macromolecule

The target, Cytochrome P450 17A1 (CYP17A1), was selected based on critical role in the production of androgens, and role in prostate cancer growth. The 3D crystallographic structure of, Cytochrome P450 17A1 (PDB ID: 6WR1) was retrieved from RCSB-protein Data Bank (https://www.rcsb.org). The structure protein consists of chain A & B (both chains consist 494 amino acids). The selection of Cytochrome P450 17A1 (CYP17A1) was justified due to its high resolution (1.85 Å), X-ray crystallographic structure in complex with HEM and AER ligands (Petrunak et al., 2023).

### 1.2 Preparation of Target Macromolecule for Molecular Docking Simulations:

For molecular docking studies, the target protein was prepared using AutoDock 4.2 in combination with MGL Tools. During the preparation process, peptide chain-B, HEM and AER ligands, heteroatoms, and water molecules were removed to obtain a clean structure. Polar hydrogens were then added, followed by the assignment of Kollman united atom charges and Gasteiger charges to ensure proper electrostatic representation. The protein structure was subsequently subjected to energy minimization to eliminate steric hindrance and achieve an optimized and stable conformation. Finally, the prepared protein was saved in PDBQT format for use in molecular docking analysis which is incorporates essential parameters like atomic charge field required for molecular docking (Morris et al., 2009).

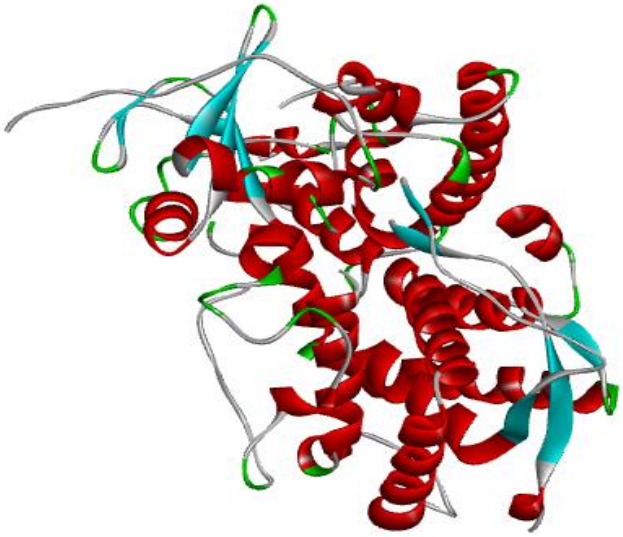

**Figure-1.** 3D crystal structure of Cytochrome P450 17A1 (CYP17A1)

### 2.3 Virtual Screening, Selection and Preparation of Ligands

Virtual screening and ligand preparation are fundamental steps in molecular docking studies, as they play a decisive role in determining the binding affinity and inhibitory potential of compounds against the target protein, Cytochrome P450 17A1. In the treatment of prostate cancer, Abiraterone is a well-established clinical inhibitor of CYP17A1 and was therefore selected as the reference ligand in this study. The two-dimensional (2D) and three-dimensional (3D) structures of Abiraterone (PubChem ID: 132971) were obtained from the PubChem database (https://pubchem.ncbi.nlm.nih.gov) in SDF format for subsequent analysis(*PubChem Compound Summary for CID 132971, Abiraterone.*, 2026)

To identify potential phytochemical inhibitors targeting CYP17A1, a virtual screening approach was carried out using the Pharmit search engine (https://pharmit.csb.pitt.edu) with ligand datasets sourced from the IMPPAT database(https://cd.imsc.res.in/imppat/).

The pharmacophore generation was initiated by uploading the target CYP17A1 (PDB ID: 6WR1) in PDB format along with the reference ligand Abiraterone in SDF format in Pharmit search engine. Careful selection of ligands is very essential for reliable pharmacophore modelling; therefore, key pharmacophoric features such as hydrogen bond donors and acceptors, aromatic ring systems, and molecular shape constraints were defined to guide the identification of potential inhibitors. To ensure drug-like properties, stringent filtering criteria were applied: molecular weight ≤ 500g/mol, rotatable bonds ≤ 10, lipophilicity (LogP) ≤ 10, polar surface area ≤ 150 Å², hydrogen-bond donors ≤ 5, and hydrogen-bond acceptors ≤ 10. Owing to its extensive and diverse phytochemical repository, the IMPPAT database was selected as the screening library. Following parameter optimization, the pharmacophore-based virtual screening was performed,

**Figure-2.** 2D structures of selected Compounds for Molecular Docking against CYP17A1

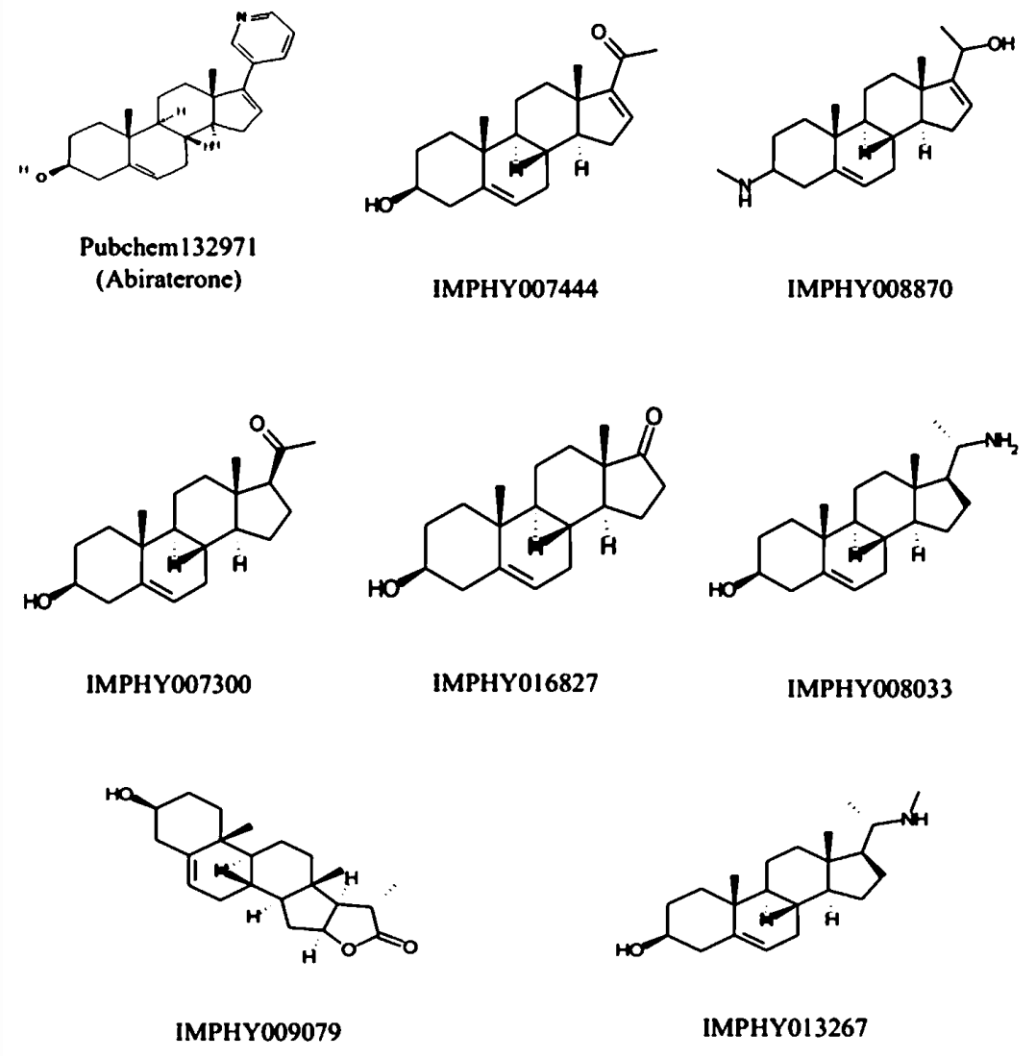


resulting in a refined set of candidate compounds that satisfied all predefined criteria and were selected for further investigation (Lipinski et al., 2001).

Following pharmacophore modelling, seven phytochemical compounds—IMPHY007444, IMPHY008870, IMPHY007300, IMPHY016827, IMPHY008033, IMPHY009079, and IMPHY013267—were identified and selected for further analysis based on their compliance with the defined screening criteria. The selected compounds were retrieved from the IMPPAT database and converted into AutoDock-compatible file formats (PDB, PDBQT, and MOL). Ligand preparation was performed using AutoDock 4.2, during which the root atoms were assigned, torsional flexibility and active rotatable bonds were defined, and the structures were subjected to energy minimization. The optimized ligands were then saved in PDBQT format for subsequent molecular docking analysis (Mohanraj et al., 2018).

### 2.4 Molecular docking simulation studies

The prepared Cytochrome P450 17A1 (PDB ID: 6WR1) was subjected to molecular docking analysis using AutoDock 4.2. A blind docking strategy was employed, utilizing a grid box of 126 × 126 × 126 points centred on the protein with a spacing of 0.497 Å, and grid center coordinates set at (25.32, 9.185, −65.115), thereby encompassing the entire protein structure to ensure comprehensive exploration of all potential ligand-binding sites. The grid parameters were saved in grid parameter file (GPF) format to maintain consistency across docking runs. Docking simulations were performed using the Lamarckian Genetic Algorithm (LGA) implemented in AutoDock 4.2, with parameters set to 10 runs, a population size of 150, a maximum of 2,500,000 energy evaluations, 27,000 generations, a mutation rate of 0.02, a crossover rate of 0.8, and an elitism value of 1. Docking parameter files (DPF) were generated, and both AutoGrid and AutoDock were executed to produce GLG and DLG output files containing detailed results, including binding energies, inhibition constants, energy components, and hydrogen-bonding interactions. The resulting protein–ligand complexes were analysed and ranked based on binding energy, and the top-ranked conformations were saved in PDB format for further protein–ligand interaction analysis (Lohning et al., 2017).

## 1. Results

### 3.1. Molecular docking, Volumetric analysis of ligand-binding site

The molecular docking study assessed the binding potential of eight compounds against the target protein, including the reference drug Abiraterone. The results showed noticeable differences in binding energies, inhibition constants, and interaction patterns, highlighting variations in ligand affinity and stability (Table 1).

**Table-1.** Binding energy values, inhibition constant, H-bonds and other interactive bonds residues information of CYP17A1 with respective phytochemicals

| S. No | Compound name (ID) | Binding energy (δg) (Kcal/Mol) | Inhibition constant | No of h-bonds | H-bonds forming residues | Hydrophobic interaction |
|---|---|---|---|---|---|---|
| 1 | Pubchem132971 (Abiraterone) | -9.59 kcal/mol | 98.14 nM | 1 | Asn202 | Ile206, Glu305, Ile205, Lue209, Val482, Thr306, Tyr201, Arg239, Gly297, Gly301, Ala302, Ala113, Phe114, Ile371, Val366, Val483, Ala367, Asp298. |
| 2 | IMPHY007444 | -9.91 kcal/mol | 54.14 nM | 1 | His373 | Arg440, Ile371, Arg96, Cys442, Thr306, Ala448, Val310, Phe435, Val366, Pr0434, Ala367, Ser441, Gly436, Lue370, Leu86, Ala437, Leu361. |
| 3 | IMPHY008870 | -10.01 kcal/mol | 46.14 nM | 3 | His373, Arg440, Arg96. | Cys442, Thr306, Thr307, Ala448, Val310, Leu452, Phe435, Leu361, Val366, Pho434, Ala367, Gly436, Leu370, Ala437, Leu86, Ser441, Ile371 |
| 4 | IMPHY007300 | -8.39 kcal/mol | 710.07nM | 3 | His373, Ile371, Arg96. | Arg440, Ser441, Cys442, Thr306, Ala302, Val310, Phe435, Val366, Ala367, Pro434, Gly436, Leu86, Leu370. |
| 5 | IMPHY016827 | -8.4 kcal/mol | 691.72 nM | 1 | His373 | Arg96, Leu86, Thr306, Val366, Cys442, Arg440, Ile371, Ser441, His373, Leu370. Ala367, Pro434. Phe435, Gly436. |
| 6 | IMPHY008033 | -9.19 kcal/mol | 183.19 nM | 2 | Arg96, Arg440 | His373, Ile371, Ala437, Ser441, Leu370, Gly436, Leu86, Ala367, Cys442, Val366, Pro434, Phe435, Leu361, Leu452, Ala448, Val310, Thr307, Yhr306. |
| 7 | IMPHY009079 | -11.39 kcal/mol | 4.96 nM | 3 | His373, Ile371, Arg96. | Leu370, Arg440, Cys442, Yhr306, Val310, Ala448, Thr307, Phe435, Leu452, Val366, Pro434, Ser441, Ala367, Ala437, Gly436. Leu86 |
| 8 | IMPHY013267 | -8.97 kcal/mol | 264.3 nM | 2 | Arg96, Arg440. | His373, Ile371, Ala367, Cys442, Thr307, Leu452, Val310, Thr306, Phe435, Ala448, Leu361, Val366, Pho434, Gly436, Leu370, Ser441. |

**CYP17A1 Binding Interaction with PubChem132971 (Abiraterone)**

The reference ligand Abiraterone exhibited a binding energy of −9.59 kcal/mol with an inhibition constant of 98.14 nM, indicating good binding affinity. It formed one hydrogen bond with ASN202, which contributed to anchoring the ligand within the binding pocket. In addition, several hydrophobic interactions with residues such as ILE206, GLU305, LEU209, VAL482, THR306, TYR201, ARG239, and PHE114 further stabilized the complex.

### 3.1.1. CYP17A1 Binding Interaction with IMPHY007444

IMPHY007444 demonstrated a slightly improved binding affinity, with a binding energy of −9.91 kcal/mol and an inhibition constant of 54.14 nM. It formed one hydrogen bond with HIS373, while multiple hydrophobic interactions involving residues such as ARG440, ILE371, ARG96, CYS442, and PHE435 enhanced its stability within the active site.

### 3.1.2. CYP17A1 Binding Interaction with IMPHY008870

IMPHY008870 showed strong binding characteristics, with a binding energy of −10.01 kcal/mol and an inhibition constant of 46.14 nM. It established three hydrogen bonds with HIS373, ARG440, and ARG96, indicating strong polar interactions. These were complemented by extensive hydrophobic contacts with residues such as CYS442, THR306, LEU452, and PHE435, resulting in a well-stabilized complex.

### 3.1.3. CYP17A1 Binding Interaction with IMPHY007300

IMPHY007300 displayed moderate binding affinity, with a binding energy of −8.39 kcal/mol and an inhibition constant of 710.07 nM. Despite forming three hydrogen bonds with HIS373, ILE371, and ARG96, the overall binding strength was lower, likely due to comparatively weaker hydrophobic interactions with residues such as ARG440, CYS442, and VAL366.

### 3.1.4. CYP17A1 Binding Interaction with IMPHY016827

IMPHY016827 showed relatively weaker binding, with a binding energy of −8.40 kcal/mol and an inhibition constant of 691.72 nM. It exhibited minimal or no hydrogen bonding, although occasional interaction with HIS373 was noted. Binding stability was mainly supported by hydrophobic interactions involving residues such as ARG96, CYS442, LEU370, and PHE435, but these were not sufficient to produce strong affinity.

### 3.1.5. CYP17A1 Binding Interaction with IMPHY008033

IMPHY008033 exhibited a binding energy of −9.19 kcal/mol and an inhibition constant of 183.19 nM, indicating moderate to good binding affinity. It formed two hydrogen bonds with ARG96 and ARG440, along with several hydrophobic interactions involving HIS373, ILE371, CYS442, VAL366, and

**Figure-1.** Binding energy values, inhibition constant, H-bonds and other interactive bonds residues information of CYP17A1 with respective phytochemicals

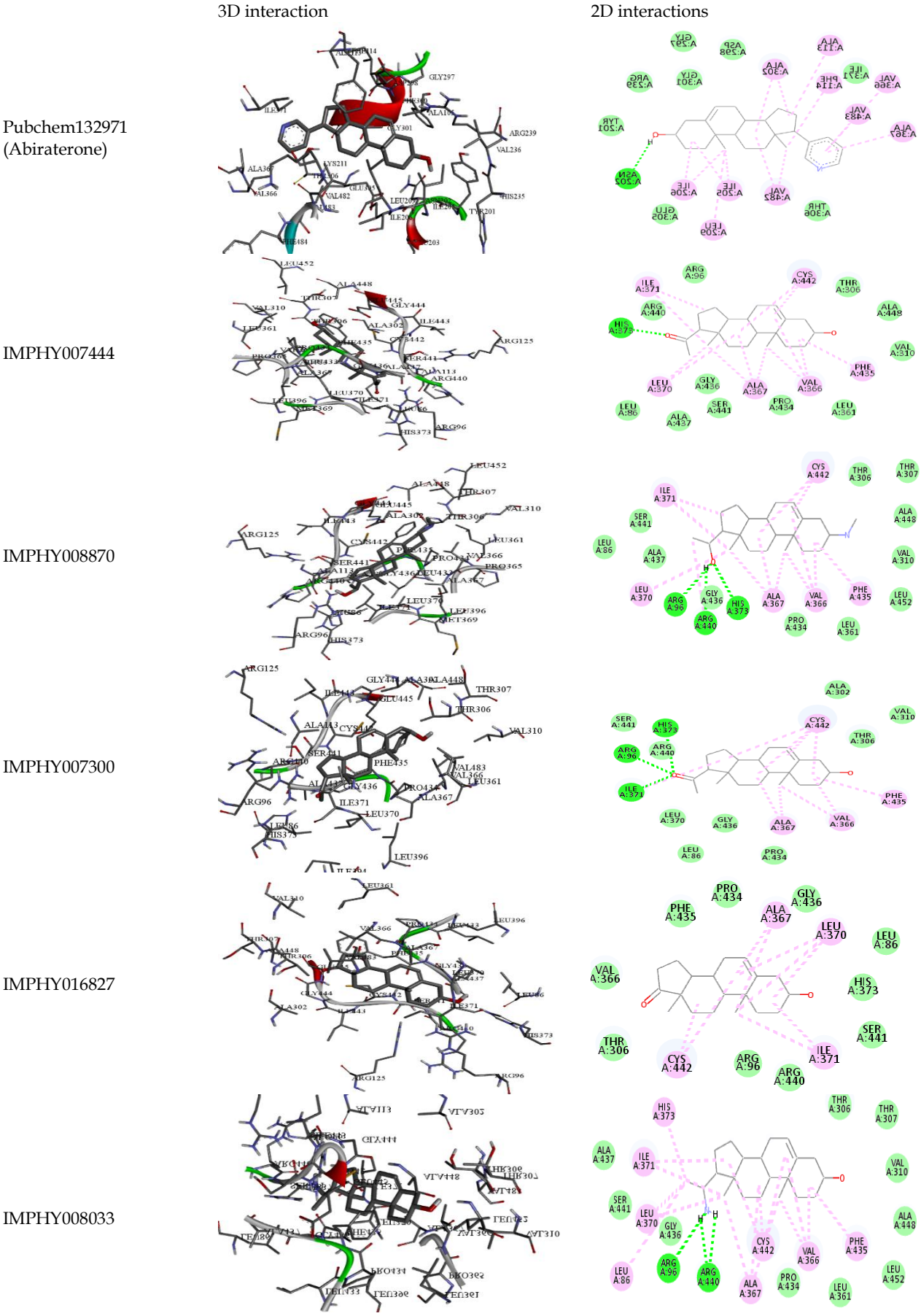

IMPHY009079

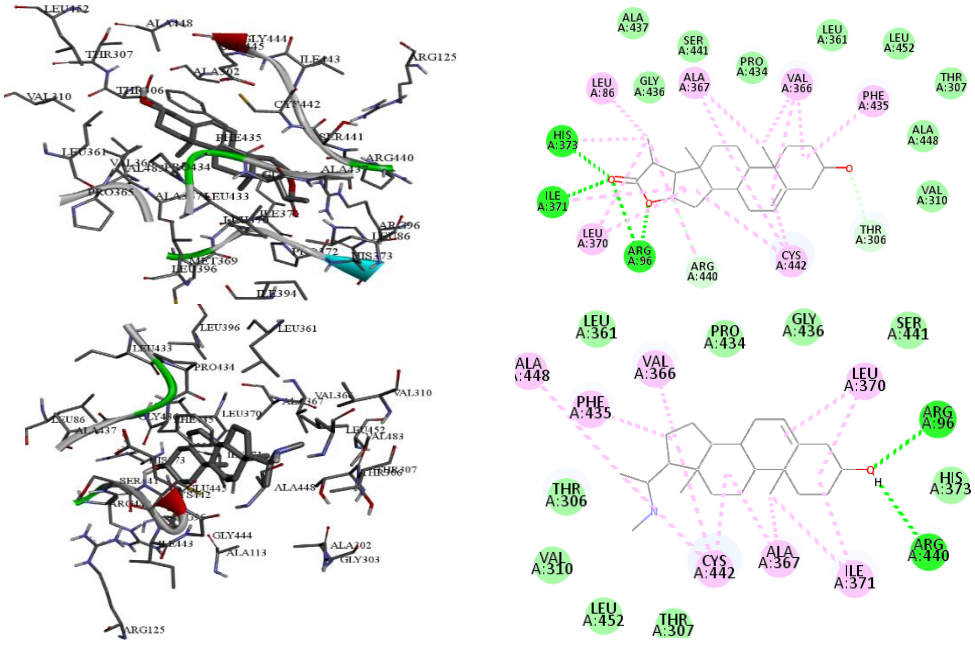

IMPHY013267

PHE435, which contributed to the overall stability of the complex.

### 3.1.6. CYP17A1 Binding Interaction with IMPHY009079

Among all tested compounds, IMPHY009079 showed the strongest binding affinity, with a binding energy of −11.39 kcal/mol and an inhibition constant of 4.96 nM. It formed three hydrogen bonds with HIS373, ILE371, and ARG96, indicating strong and specific interactions within the binding site. These were further reinforced by extensive hydrophobic contacts with residues such as LEU370, ARG440, CYS442, VAL310, LEU452, and PHE435, suggesting a highly stable and favourable binding conformation.

### 3.1.7. CYP17A1 Binding Interaction with IMPHY013267

IMPHY013267 demonstrated moderate binding affinity, with a binding energy of −8.97 kcal/mol and an inhibition constant of 264.3 nM. It formed two hydrogen bonds with ARG96 and ARG440, while hydrophobic interactions with residues such as HIS373, CYS442, VAL310, LEU452, and PHE435 contributed to maintaining the ligand within the active site.

## 3.2. Analysis of Molecular Docking Results

The molecular docking study evaluated eight ligands—consisting of Abiraterone and seven Phytochemicals—against the target protein binding site. These simulations, conducted using a blind docking approach and the Lamarckian Genetic Algorithm, revealed significant variations in binding affinities and interaction patterns among the tested compounds12. The results highlight a diverse landscape of molecular recognition, with inhibition constants spanning from low nanomolar to high micromolar ranges.

### 3.2.1. Binding Affinity and Inhibition Potential

The docking results demonstrated a broad range of binding energies, extending from -8.39 kcal/mol to -11.39 kcal/mol. Notably, IMPHY009079 (Compound 7) emerged as the lead candidate, demonstrating superior binding characteristics with a remarkably low energy of -11.39 kcal/mol and a highly potent inhibition constant (*Ki*) of 4.96 nM. This indicates an exceptionally strong affinity for the target receptor, significantly outperforming other high-performing candidates such as IMPHY008870 (-10.01 kcal/mol, = 46.14 nM) and IMPHY007444 (-9.91 kcal/mol, = 54.14 nM). Conversely, IMPHY007300 displayed the weakest binding energy at -8.39 kcal/mol, corresponding to a much higher inhibition constant of 710.07 nM, which illustrates how subtle structural variations within the phytochemicals influence inhibitory potency.

### 3.2.2. Hydrogen Bonding and Residue Interactions

Hydrogen bonding played a pivotal role in stabilizing the ligand-protein complexes, though the data suggests that H-bond count alone is not the sole determinant of affinity. The most effective inhibitor, IMPHY009079, established three hydrogen bonds with residues HIS373, ILE371, and ARG96. Interestingly, IMPHY007300 also formed three hydrogen bonds with these same residues but resulted in a significantly weaker binding energy, highlighting that the spatial orientation and electronic complementarity of these contacts are critical for stability. Specific residue involvement across the set identifies HIS373 as a primary anchor point, as it interacted with five of the eight ligands. Other recurring polar contacts included ARG96 and ARG440, which were consistently involved in stabilizing the more potent inhibitors.

### 3.2.3. Structural Insights and Binding Mode Analysis

The structural analysis confirms that while polar contacts provide specificity, a robust network of hydrophobic interactions drives overall binding stability and cavity occupancy. Top-performing ligands like IMPHY009079 and IMPHY008870 engaged in extensive non-polar contacts with residues such as VAL366, ALA367, PHE435, and CYS442. The involvement of residues like LEU370, PRO434, and THR306 suggests that these compounds achieve high steric complementarity within the binding pocket. In contrast, Pubchem132971 utilized a distinct set of residues, including TYR201 and VAL482, indicating an alternative sub pocket targeting strategy compared to the phytochemicals. These

findings suggest that the most successful inhibitors combine a rigid scaffold with optimized hydrophobic packing to minimize entropic penalties during the binding process.

#### 3.2.4. Comparative Pharmacological Implications

The pharmacological potential of the leading candidates is significant, as their nanomolar values—particularly the 4.96 nM observed for IMPHY009079—predict high *in vivo* efficacy4. The synergy of strategic hydrogen bonding at key anchor residues like HIS373 and ARG96 with extensive hydrophobic filling demonstrates an optimal interaction profile. These insights provide a robust computational foundation for prioritizing these specific scaffolds for further synthesis and experimental validation. The identified candidates show promise in overcoming current therapeutic limitations, offering a clear blueprint for the development of next-generation inhibitors with improved binding characteristics and potential clinical advantages.

## 4. Discussion

The present study highlights the potential of phytochemical scaffolds as inhibitors of CYP17A1, a critical enzyme in androgen biosynthesis and prostate cancer progression. Compare to FDA approved Abiraterone drug, several compounds showing best binding strength. Particularly noteworthy is our lead compound's interactions with ASN202, ILE206, GLU305, ILE205, LUE209, VAL482, THR306 and other residues, and which corroborates the findings of (Fehl et al., 2018; Gujjeti et al., 2014; Gurrapu et al., 2017; Janakiramulu et al., 2025), regarding this residue's crucial role in Androgen biosynthesis and prostatic growth. we observed that compounds with more hydrogen bonds and stronger hydrophobic interactions compare to Abiraterone drug, such as our top-performing ligand, achieved superior binding energies. So, the results support the game changer in drug discovery via targeting CYP17A1 highlighted in recent reviews.

When compared to other docking studies targeting prostate cancer proteins, the results are particularly striking. For example, (Morla Madhav & Mamidala Estari, 2025; Al-Masri et al., 2024; Namthabad et al., 2014; Swapna et al., 2024) reported their lead AR inhibitor with a binding energy of –9.28 kcal/mol and $K_i$ of 156.89 nM. The markedly lower inhibition constant of IMPHY009079 against CYP17A1 suggests that phytochemical scaffolds may achieve superior efficacy by exploiting the unique structural features of CYP17A1 rather than AR antagonism alone. This observation aligns with the therapeutic rationale that CYP17A1 inhibition directly disrupts androgen biosynthesis, thereby addressing the root cause of prostate cancer progression.

A recurring theme across docking studies is that hydrogen bond count alone does not predict binding strength. In the CYP17A1 docking results, IMPHY009079 and IMPHY007300 both established three hydrogen bonds with residues HIS373, ILE371, and ARG96, yet their binding energies differed by exactly 3.0 kcal/mol. This observation directly mirrors the findings in the AR study, where Compound with fewer hydrogen bonds but stronger hydrophobic packing achieved superior affinity. These findings emphasize that spatial orientation, electronic complementarity, and hydrophobic stabilization are more decisive factors than hydrogen bond number in determining inhibitory potency. The structural specificity of the CYP17A1 binding site is defined by a unique set of anchor residues, primarily HIS373, which was involved in stabilizing five of the eight tested ligands. While the targets differ, the reliance on hydrophobic packing to drive stability is a commonality. In the CYP17A1 results, the lead compound engaged an extensive network of residues, including VAL366, ALA367, PHE435, and CYS442.

the present docking study demonstrates that phytochemical scaffolds, particularly IMPHY009079, exhibit exceptional inhibitory potential against CYP17A1. The comparative analysis of docking studies, benchmark drugs, and other CYP17A1 docking works underscores the promise of these compounds as next-generation inhibitors. The synergy between targeted hydrogen bonding and extensive hydrophobic stabilization provides a strong computational foundation for advancing these phytochemicals toward experimental validation and clinical development in prostate cancer therapy. Translating there in-silico results to clinical efficacy required to potential metabolic stability issues common to high-affinity compounds. Future work should incorporate the molecular dynamics approaches recommended to assess binding stability under physiological conditions. these findings of this study contribute to the growing body of evidence supporting structure-based design of CYP17A1-targeting based prostate cancer therapeutics, while highlighting the need for preclinical evaluation of compounds

## 5. Conclusion

This molecular docking study demonstrates the significant potential of phytochemicals as inhibitors of CYP17A1, a key enzyme involved in androgen biosynthesis and prostate cancer progression. Several compounds exhibited binding affinities comparable to or exceeding the FDA-approved drug Abiraterone, with IMPHY009079 emerging as the most promising candidate. It showed a binding energy of –11.39 kcal/mol and an inhibition constant of 4.96 nM, indicating strong potency supported by key hydrogen bonding interactions within the active site. The identification of multiple nanomolar-range inhibitors highlights the therapeutic promise of phytochemical scaffolds as next-generation CYP17A1 inhibitors. By targeting androgen biosynthesis directly, these compounds offer a potential strategy for improved prostate cancer treatment. Furthermore, these findings provide a solid computational basis for future studies, including molecular dynamics simulations, ADMET analysis, and experimental validation, supporting the development of plant-derived therapeutics in precision oncology.

## Competing interests:

The authors declare that they have no competing interests

**Funding:** No funding was received for this study

## References

[1] Alex, A. B., Pal, S. K., & Agarwal, N. (2016). CYP17 inhibitors in prostate cancer: latest evidence and clinical potential. *Therapeutic Advances in Medical Oncology*, *8*(4), 267–275.

[2] Fehl, C., Vogt, C. D., Yadav, R., Li, K., Scott, E. E., & Aubé, J. (2018). Structure-Based Design of Inhibitors with Improved Selectivity for Steroidogenic Cytochrome P450 17A1 over Cytochrome P450 21A2. *Journal of Medicinal Chemistry*, *61*(11), 4946–4960.

[3] Filho, A. M., Laversanne, M., Ferlay, J., Colombet, M.,

Piñeros, M., Znaor, A., Parkin, D. M., Soerjomataram, I., & Bray, F. (2025). The GLOBOCAN 2022 cancer estimates: Data sources, methods, and a snapshot of the cancer burden worldwide. *International Journal of Cancer*, *156*(7), 1336–1346. https://doi.org/10.1002/ijc.35278

[4] Kmeťová Sivoňová, M., Jurečeková, J., Tatarková, Z., Kaplán, P., Lichardusová, L., & Hatok, J. (2017). The role of CYP17A1 in prostate cancer development: structure, function, mechanism of action, genetic variations and its inhibition. *General Physiology and Biophysics*, *36*(05), 487–499. https://doi.org/10.4149/gpb_2017024

[5] Lipinski, C. A., Lombardo, F., Dominy, B. W., & Feeney, P. J. (2001). Experimental and computational approaches to estimate solubility and permeability in drug discovery and development settings 1PII of original article: S0169-409X(96)00423-1. The article was originally published in Advanced Drug Delivery Reviews 23 (1997) 3–25. 1. *Advanced Drug Delivery Reviews*, *46*(1–3), 3–26. https://doi.org/10.1016/S0169-409X(00)00129-0

[6] Lohning, A. E., Levonis, S. M., Williams-Noonan, B., & Schweiker, S. S. (2017). A Practical Guide to Molecular Docking and Homology Modelling for Medicinal Chemists. *Current Topics in Medicinal Chemistry*, *17*(18), 2023–2040. https://doi.org/10.2174/1568026617666170130110827

[7] Mohanraj, K., Karthikeyan, B. S., Vivek-Ananth, R. P., Chand, R. P. B., Aparna, S. R., Mangalapandi, P., & Samal, A. (2018). IMPPAT: A curated database of Indian Medicinal Plants, Phytochemistry And Therapeutics. *Scientific Reports*, *8*(1), 4329.

[8] Morla Madhav, & Mamidala Estari. (2025). In silico molecular docking studies for identify to potential androgen receptor blocking agents to treat prostate cancer. *RECENT TRENDS IN ANIMAL BIOTECHNOLOGY (RTAB-2024)*, 117–126.

[9] Morris, G. M., Huey, R., Lindstrom, W., Sanner, M. F., Belew, R. K., Goodsell, D. S., & Olson, A. J. (2009). AutoDock4 and AutoDockTools4: Automated docking with selective receptor flexibility. *Journal of Computational Chemistry*, *30*(16), 2785–2791.

[10] Mortezavi, A., Salemi, S., Kranzbühler, B., Gross, O., Sulser, T., Simon, H.-U., & Eberli, D. (2019). Inhibition of autophagy significantly increases the antitumor effect of Abiraterone in prostate cancer. *World Journal of Urology*, *37*(2), 351–358. https://doi.org/10.1007/s00345-018-2385-5

[11] Omoboyowa, D. A., Balogun, T. A., Saibu, O. A., Chukwudozie, O. S., Alausa, A., Olubode, S. O., Aborode, A. T., Batiha, G. E., Bodun, D. S., & Musa, S. O. (2022). Structure-based discovery of selective CYP17A1 inhibitors for Castration-resistant prostate cancer treatment. *Biology Methods and Protocols*, *7*(1). https://doi.org/10.1093/biomethods/bpab026

[12] Petrunak, E. M., Bart, A. G., Peng, H.-M., Auchus, R. J., & Scott, E. E. (2023). Human cytochrome P450 17A1 structures with metabolites of prostate cancer drug abiraterone reveal substrate-binding plasticity and a second binding site. *Journal of Biological Chemistry*, *299*(3), 102999. https://doi.org/10.1016/j.jbc.2023.102999

[13] *PubChem Compound Summary for CID 132971, Abiraterone.* (2026). National Center for Biotechnology Information. https://pubchem.ncbi.nlm.nih.gov/compound/Abiraterone

[14] Rebello, R. J., Oing, C., Knudsen, K. E., Loeb, S., Johnson, D. C., Reiter, R. E., Gillessen, S., Van der Kwast, T., & Bristow, R. G. (2021). Prostate cancer. *Nature Reviews. Disease Primers*, *7*(1), 9. https://doi.org/10.1038/s41572-020-00243-0

[15] Schafer, E. J., Laversanne, M., Sung, H., Soerjomataram, I., Briganti, A., Dahut, W., Bray, F., & Jemal, A. (2025). Recent Patterns and Trends in Global Prostate Cancer Incidence and Mortality: An Update. *European Urology*, *87*(3), 302–313.

[16] Wróbel, T. M., Rogova, O., Sharma, K., Rojas Velazquez, M. N., Pandey, A. V, Jørgensen, F. S., Arendrup, F. S., Andersen, K. L., & Björkling, F. (2022). Synthesis and Structure-Activity Relationships of Novel Non-Steroidal CYP17A1 Inhibitors as Potential Prostate Cancer Agents. *Biomolecules*, *12*(2).

[17] Al-Masri, A. A., Ameen, F., Davella, R., & Mamidala, E. (2024). Antidiabetic effect of flavonoid from Rumex vesicarius on alloxan induced diabetes in male albino Wistar rats and its validation through in silico molecular docking and dynamic simulation studies. *Biotechnology and Genetic Engineering Reviews*, *40*(4), 4479-4494.

[18] Gujjeti, R. P., Namthabad, S., & Mamidala, E. (2014). HIV-1 reverse transcriptase inhibitory activity of Aerva lanata plant extracts. *BMC Infectious Diseases*, *14*(Suppl 3), P12.

[19] Gurrapu, S., & Mamidala, E. (2017). In Vitro HIV-1 reverse transcriptase inhibition of andrographolide isolated from Andrographis paniculata. *European Journal of Biomedical*, *4*(12), 516-522.

[20] Janakiramulu, P., & Mamidala, E. (2025). Molecular Docking and dynamic simulation analysis of flavonoid derivatives as COX-2 inhibitors. *In Silico Pharmacology*, *13*(2), 59.

[21] Namthabad, S., & Mamidala, E. (2014). Molecular docking of HIV-1 protease using alkaloids from tinospora cordifolia. *Int J Res Appl*, *1*(1), 12-6.

[22] Swapna, K., Srujana, M., & Mamidala, E. (2024). Identification of steroidal cardenolides from *Calotropis procera* as novel HIV-1 PR inhibitors: A molecular docking & molecular dynamics simulation study. *The Indian journal of medical research*, *160*(1), 78.

[23] Lunavath, V., & Mamidala, E. (2013). Preliminary phytochemical screening and antibacterial studies of the leaves of Eclipta alba (L). *Int J Pharma Biosci*, *4*, 380-4.

[24] Kumar, M. P., Mamidala, E., Al-Ghanim, K., Al-Misned, F., Ahmed, Z., & Mahboob, S. (2020). Effects of D-Limonene on aldose reductase and protein glycation in diabetic rats. Journal of King Saud University-Science, 32(3), 1953-1958.

[25] Porika, R., Poojari, S., Lunavath, V., & Mamidala, E. (2014). Preliminary phytochemical investigation and TLC analysis of P. angulata fruit extract. Journal of Pharmacy and Biological Sciences, 9(2), 11-14.

[26] Kumar Thatipamula, R., Narsimha, S., Battula, K., Chary, V. R., Mamidala, E., & Reddy, N. V. (2017). Synthesis, anticancer and antibacterial evaluation of novel (isopropylidene) uridine-[1, 2, 3] triazole hybrids. Journal of Saudi Chemical Society, 21(7), 795-802.

[27] Poojari, S., Porika, R., & Mamidala, E. (2014). Phytochemical analysis and in vitro antidiabetic activities of Physalis angulata fruit extracts. *Natl. J. Integr. Res. Med*, *5*, 34-38.

[28] Mamidala, E., Davella, R., Gurrapu, S., & Shivakrishna, P. (2020). In silico identification of clinically approved medicines against the main protease of SARS-CoV-2, causative agent of covid-19. *arXiv preprint arXiv:2004.12055*.